Event-based color change pixel in standard CMOS

Raphael Berner and Tobi Delbruck
Institute of Neuroinformatics, University of Zurich and ETH Zurich, Switzerland

***Abstract*—This paper describes a novel dichromatic spiking pixel circuit that reacts to color change but not to intensity change. It is built in standard CMOS using a buried double junction to sense wavelength information. The pixel can detect light wavelength changes of about 14nm, while not responding to intensity steps of at least a factor of three. The pixel is suitable for integration into an array and can easily be combined with a temporal log intensity contrast change pixel.**

I. Introduction

In recent years, various spike based optical sensors have been presented [1]–[6]. Several publications show that these sensors can be very useful due to their pixel-parallel preprocessing, which reduces latency and the load on subsequent processing stages [7]–[9].

These sensors are all gray scale (monochromatic). However, for some applications color information would be very useful, for example to distinguish shadows from real objects. But work on spiking color sensors has been rare, to our knowledge only one multi-pixel spiking color sensor has been presented so far [10]. However this work has the serious disadvantages of relying on an external ADC, pixels showing considerable mismatch and being slow to respond in low light situations.

Using standard CMOS color imagers with color filters for low power applications has the disadvantage that the Bayer decomposition algorithm needs a substantial amount of processing power. Employing the wavelength-dependent absorption length in silicon for color detection has been proposed in the eighties [11], [12], and many different circuits which employ this principle have been published [10], [13]–[15]. Using this property for color imaging requires special process steps to achieve sufficient image quality [16], but we believe some basic wavelength separation capability is sufficient for many vision tasks, which is supported by the fact that most animals are only dichromats [17].

This paper presents a novel circuit that detects changes in wavelength, much as the DVS [1] detects changes in log intensity. The pixel employs a buried double junction (BDJ) to achieve dichromatic color sensitivity in standard CMOS. The pixel asynchronously emits events indicating whether the mean wavelength of the incident light has increased or decreased, i.e. whether the light has become bluer or redder.

The circuit relies on MOS transistors running in subthreshold to have an exponential current-voltage relationship and be low power, so it can be used in an array.

II. The Buried Double Junction

The buried double junction (BDJ) is a stack of two photodiodes formed by the active-well and well-substrate junctions, which is available in any CMOS process (Fig. 1). Because the absorption length of photons in silicon increases monotonically with wavelength [18], [19], the two junctions have different spectral responses, which is shown in Fig. 2 for the 0.5um 3M 2P process used. The bumps in the curves probably stem from reflections in the oxide [20].

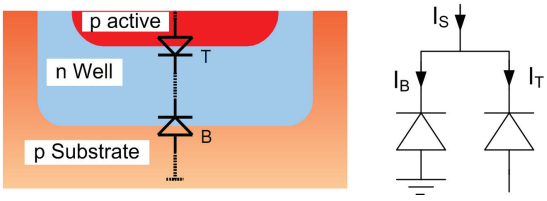

Fig. 1. Illustration and schematic of the buried double junction.

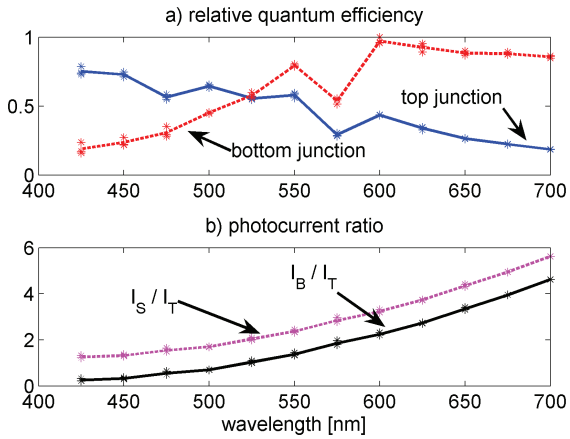

Fig. 2. Spectral response of the BDJ in the $0.5\mu m$ process used, measured with test structures on the same die as the test pixel. a) The relative quantum efficiency (normalized to the maximum value) of the top (blue, solid) and bottom (red, dashed) junction. b) Ratio of the photocurrents; the solid line shows the ratio between the junction currents; the dashed line shows the ratio of the available currents I_S/I_T.

A disadvantage of the BDJ is that only the currents I_T and $I_S = I_T + I_B$ are accessible for continuous time circuits, but not I_B directly. Fu and Titus [15] try to address this by subtracting a copy of I_T from I_S. This is problematic due to transistor mismatch and may work for a single pixel, but will cause very different pixel responses across an array.

As can be seen from figure 2, I_S/I_T varies almost a factor of five in the visible range. We think this is sufficient for change detection, and therefore our pixel circuit works directly on I_T and I_S, which makes it more suitable for using in an array, as no mismatch-prone current copying is involved.

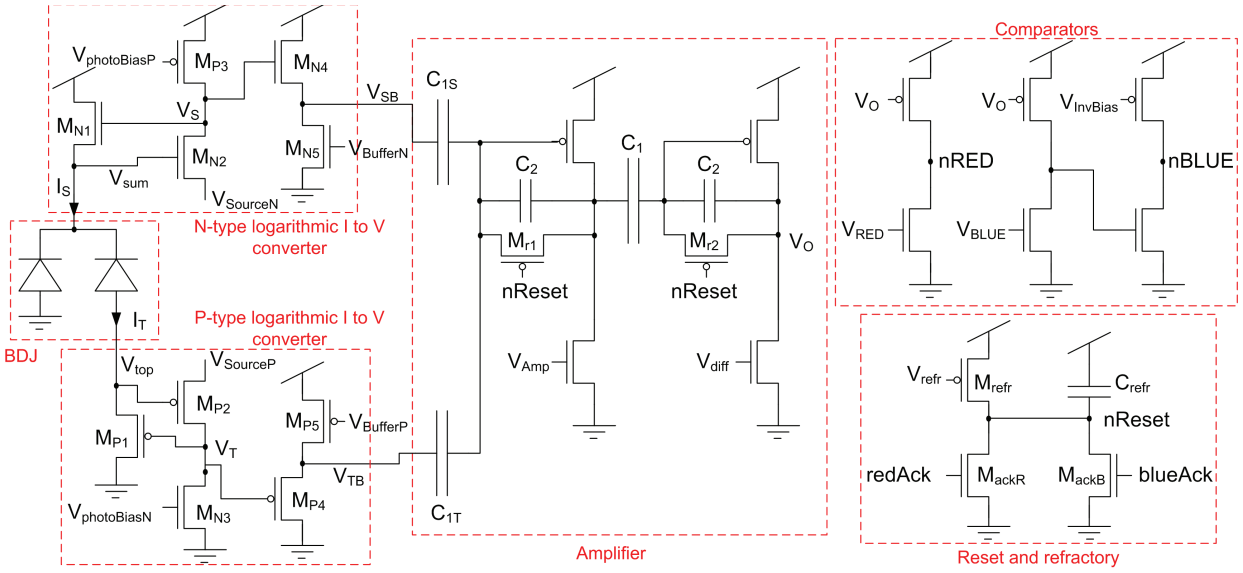

Fig. 3. Complete pixel circuit. V_{sourceN} and V_{sourceP} are source biases used to ensure proper biasing of the BDJ.

III. Pixel Circuit

The pixel circuit (Fig. 3) consists of a BDJ, two logarithmic current to voltage converters, a two-stage summing amplifier, two simple comparators and a reset and refractory circuit. Whenever the pixel crosses threshold, the summing amplifier is reset by closing the switches M_{r1} and M_{r2}, thereby memorizing the last value. The pixel computes the difference of the logarithms of I_S and I_T.

The voltage V_S is

$$V_S = \frac{1}{\kappa_{N1}} \left(V_{sum} + U_T \ln \frac{I_S}{I_{0N1}} \right), \tag{1}$$

where U_T is the thermal voltage kT/q and κ the subthreshold slope factor. V_{sum} is nearly constant if the gain of the common source amplifier formed by M_{N2} and M_{P3} is sufficient [1], [19]. V_S is buffered by a source follower.

$$V_{SB} = \frac{\kappa_{N4}}{\kappa_{N1}} V_{sum} - \kappa_{N5} V_{\mathrm{BufferN}} + \frac{\kappa_{N4}}{\kappa_{N1}} \ln \frac{I_S}{I_{0N1}}. \tag{2}$$

If κ_{N4} is equal to κ_{N1}, then

$$V_{SB} = U_T \ln \frac{I_S}{I_{0N1}} + V_{sum} - \kappa_{N5} V_{\mathrm{BufferN}} \tag{3}$$

$$\tag{4}$$

The p-type front-end works in a similar way, resulting in an output voltage

$$V_{TB} = V_{DCp} - \frac{\kappa_{P4}}{\kappa_{P1}} U_T \ln \frac{I_T}{I_{0P1}}, \tag{5}$$

which, for for $\kappa_{P4} = \kappa_{P1}$, simplifies to

$$V_{TB} = -U_T \ln \frac{I_T}{I_{0P1}} + V_{DCp}. \tag{6}$$

The summing amplifier is implemented as two consecutive capacitive-feedback inverting amplifiers, where the first one has two input capacitances C_{1T} and C_{1S}. The first stage of the amplifier is used to limit the bandwidth of the pixel to balance possible bandwidth differences in the two front-ends by adjusting the bias voltage V_{amp}. The gain of each stage is C_1/C_2, resulting in a total gain $A = (C_1/C_2)^2$.

The output of the summing amplifier is therefore

$$\Delta V_{out} = A \cdot U_T \left(\Delta \ln \frac{I_S}{I_{0N1}} - \Delta \ln \frac{I_T}{I_{0P1}} \right) \tag{7}$$

$$= A \cdot U_T \left(\Delta \ln \frac{I_S}{I_T} + \Delta \ln \frac{I_{0P1}}{I_{0N1}} \right) \tag{8}$$

$$= A \cdot U_T \cdot \Delta \ln \left(\frac{I_S}{I_T} \right), \tag{9}$$

which responds only to changes in the ratio of the photocurrents, but not to changes in intensity only. But because κ_{X4} is not exactly equal to κ_{X1}, and κ is slightly current dependent, some response to intensity changes will result.

In this design, the junction leakage of the reset switch of the first stage is amplified by the second stage. Therefore we use C_1/C_2 switches in the second stage to approximately balance the leakage of the first stage.

The comparators compare the output of the amplifier against two thresholds V_{BLUE} and V_{RED} that are offset from the reset voltage V_{diff} to detect increasing and decreasing changes. If the input of a comparator overcomes its threshold, a BLUER or REDDER event is generated. The output of the BLUE comparator is followed by a starved inverter to generate active low signals for both types of events.

These signals *nBLUE* and *nRED* are connected to the arbiter [21], and when the pixel is acknowledged, V_{nReset} is pulled to ground by M_{ackB} or M_{ackR}, thereby closing the reset switches M_{r1} and M_{r2}. The transistors M_{ackB} and M_{ackR} also enable an adjustable refractory period (implemented by M_{refr} and C_{refr}), which limits the maximum firing rate.

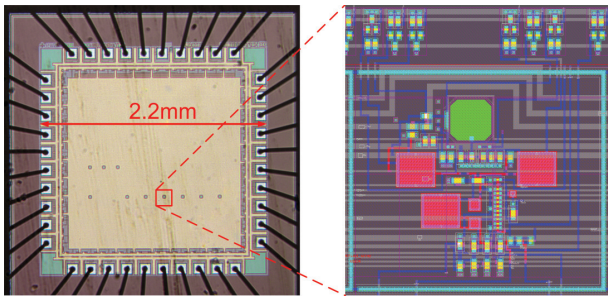

Fig. 4. Test chip die photo and pixel layout with local buffers. Metal3 is used to shield the circuits from light. In the die photo, the openings in metal3 for the photodiodes can be seen. The layout of the circuits was not optimized for area.

TABLE I
TEST-CHIP SPECIFICATIONS

Process	AMI $0.5\mu m$, N-Well, 3 Metal, 2 Poly
Die Area	$2.2mm \times 2.2mm$
Photodiode Area	$690\mu m^2$
Number of elements per pixel	25 transistors, 6 capacitors
Nominal Amplifier Gain	40dB
Actual Amplifier Gain	38.6dB
V_O noise	$32.5mV$ RMS

IV. TEST CHIP

A test chip was fabricated through the MOSIS service in an AMI $0.5\mu m$ 3M 2P process. Table I lists some specifications and Fig 4 shows a die photo and the pixel layout. The test chip includes structures to measure photocurrents, as well as different test pixel designs.

The capacitances C_1 and C_2 were designed to be $500fF$ and $50fF$ respectively, resulting in a nominal amplifier gain of $A = 100$.

V. MEASUREMENT RESULTS

For the measurements, we stimulated the test pixel with a red and a blue LED. To measure the response to intensity changes, the blue diode was stimulated with a sinusoidal current alone, while the red LED was off. To measure the response to a change in wavelength, we stimulated the pixel with the two LEDs simultaneously, where the current of the red LED was held constant, while the blue one was varied sinusoidally, which results in light color changes from blue to red. Because the photocurrents are linear with intensity, this has the same effect as stimulating with a single monochromatic light source.

Fig. 5 shows scope traces demonstrating the basic property of the pixel. Fig. 5 a) shows the response to intensity change, where the topmost (blue) curve is the amplifier output voltage V_O which shows very little response. In Fig. 5 b) however, where the light color changes as well, the output voltage V_O responds with high amplitude. It can also be seen that in the top curve V_{SB} and V_{TB} respond with higher amplitude than in the bottom curve, because the intensity change is bigger.

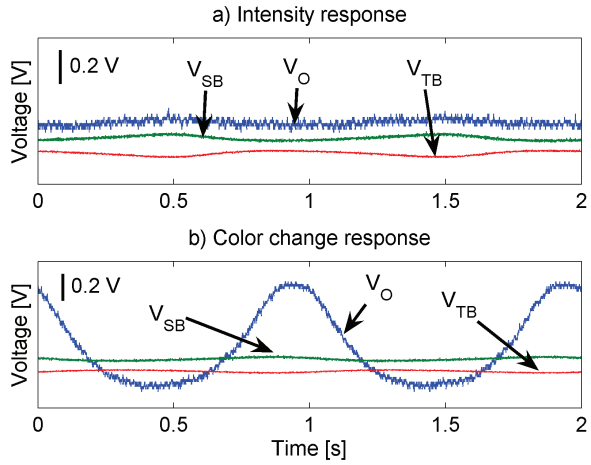

Fig. 5. Scope traces. a) shows the output of the chip when stimulated with only the blue LED (wavelength 430nm, intensity changes a factor of 6.37). b) shows the response when the red LED is added with a constant voltage (mean wavelength changes between 475nm and 550nm, intensity changes a factor of 3.73). The traces show from top to bottom: amplifier output voltage V_O, V_{SB}, V_{TB}. All traces have arbitrary offsets added for display and the thresholds are set very high to prevent the pixel from spiking.

But because the ratio of the currents stays the same, the sum of V_{SB} and V_{TB} is nearly constant.

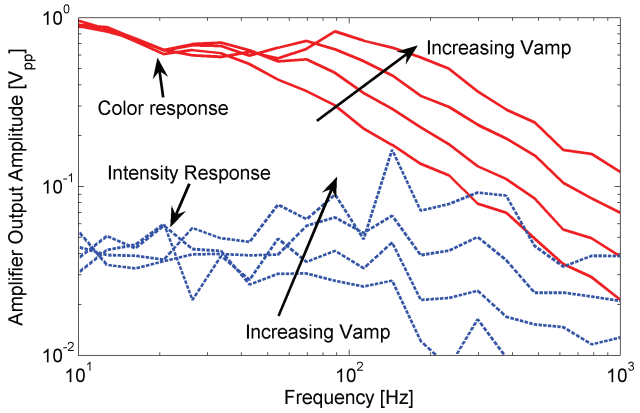

Fig. 6. Frequency response when stimulated with only the blue LED, (wavelength 430nm, intensity changes a factor of 11.7 (approximately 4.5 to $0.38Wm^{-2}$)) and when the red LED is added with a constant voltage (mean wavelength changes between 460nm and 543nm, intensity changes a factor of 6.3 (approximately 4.7 to $0.75Wm^{-2}$)). The traces show the amplitude of the output voltage V_O for different bias voltages V_{amp}, which changes the amplifier cutoff frequency. The thresholds are set very high to prevent the pixel from spiking.

Fig. 6 shows the temporal frequency response, both for intensity change only (dashed) and for color change (solid). It also shows that the circuit responds much more to color change than to intensity change only. For intensity change, the output amplitude increases above 100Hz for high bias currents, because the dynamics of the two front-ends are not perfectly matched since they are approximately proportional to absolute photocurrent. Limiting the bandwidth is therefore essential. Adaptive biasing of V_{amp} would be beneficial to achieve faster operation in well illuminated conditions.

The sensitivity of the pixel to wavelength changes was measured by applying voltages to the red and blue LEDs, so that wavelength changes of $\pm 10nm$ resulted. The sensitivity is highest in the blue and drops towards red (Fig. 7). Given the relatively high noise levels, the threshold should be set at least $100mV$ away from V_{diff}. The minimal wavelength change which can be detected is therefore around $9nm$ in the blue range and around $14nm$ in the red.

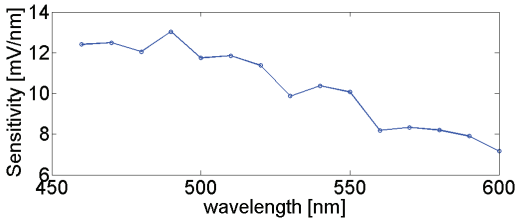

Fig. 7. Wavelength change sensitivity.

Fig. 8 shows spike raster plots comparing the color pixel presented in this work to a log intensity change pixel [1] with the same two stage amplifier as the color pixel, using a well-substrate photodiode. The thresholds are set about $120mV$ away from V_{diff}. In fig. 8 a), with intensity change of a factor of 2.4, the color pixel does not respond. In the case of color change however, the color pixel responds, while the log intensity pixel still responds, even though a bit less than in the intensity case.

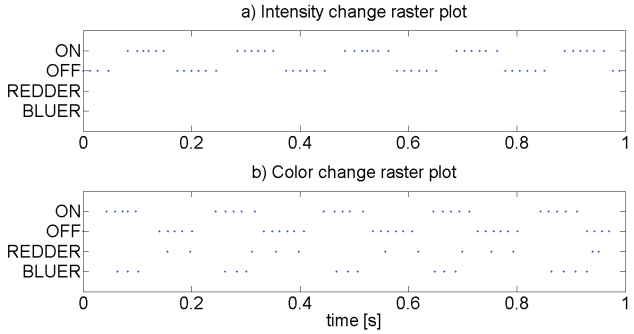

Fig. 8. Raster plot which show comparison between intensity contrast change and color change pixel. ON an OFF events are the output of the log intensity change pixel, REDDER and BLUER events from the color change pixel.

VI. Discussion and Outlook

This work demonstrates successfully how the BJD can be used to create a neuromorphic spiking color sensor. However the reset circuit has to be improved by using separate signals for M_{r1} and M_{r2} to avoid the amplification of the charge injection due to M_{r1}, by holding the second stage slightly longer in reset. In this test pixel the refractory bias V_{refr} has to be set quite close to V_{DD} so that the switches close slowly, which reduces the effect of charge injection.

This color change pixel can easily be combined with the intensity change pixel used in the DVS [1] and share the same photodiode and n-type current-to-voltage converter.

Acknowledgment

This project was supported by the Swiss National Science Fund grant 200021-112354 / 1, the University of Zurich and ETH Zurich.

References

[1] P. Lichtsteiner, C. Posch, and T. Delbruck, "A 128×128 120dB 15us Latency Asynchronous Temporal Contrast Vision Sensor," *IEEE Journal of Solid State Circuits*, vol. 43, pp. 566–576, Feb. 2007.

[2] P. F. Ruedi, P. Heim, F. Kaess, E. Grenet, F. Heitger, P. Y. Burgi, S. Gyger, and P. Nussbaum, "A 128 128 pixel 120-dB dynamic-range vision-sensor chip for image contrast and orientation extraction," *IEEE Journal of Solid-State Circuits*, vol. 38, no. 12, pp. 2325–2333, 2003.

[3] X. Qi, X. Guo, and J. G. Harris, "A time-to-first spike CMOS imager," in *Circuits and Systems, 2004. IEEE International Symposium on*, 2004, pp. 23–26.

[4] J. Lenero-Bardallo, T. Serrano-Gotarredona, and B. Linares-Barranco, "A mismatch calibrated bipolar spatial contrast AER retina with adjustable contrast threshold," in *Circuits and Systems, 2009. IEEE International Symposium on*, 2009, pp. 1493–1496.

[5] E. Culurciello, R. Etienne-Cummings, and K. Boahen, "A biomorphic digital image sensor," *IEEE Journal of Solid-State Circuits*, vol. 38, no. 2, pp. 281–294, 2003.

[6] M. Azadmehr, J. P. Abrahamsen, and P. Häfliger, "A Foveated AER Imager Chip," in *Circuits and Systems, 2005. IEEE International Symposium on*, 2005, pp. 2751–2754.

[7] C. Shoushun, B. Martini, and E. Culurciello, "A bio-inspired event-based size and position invariant human posture recognition algorithm," in *Circuits and Systems, 2009. IEEE International Symposium on*, 2009, pp. 775–778.

[8] F. Zhengming, T. Delbruck, P. Lichtsteiner, and E. Culurciello, "An Address-Event Fall Detector for Assisted Living Applications," *IEEE Trans. on Biomedical Circuits and Systems*, vol. 2, pp. 88–96, 2008.

[9] J. Conradt, M. Cook, R. Berner, P. Lichtsteiner, R. Douglas, and T. Delbruck, "A pencil balancing robot using a pair of AER dynamic vision sensors," in *Circuits and Systems, 2009. IEEE International Symposium on*, 2009, pp. 781–784.

[10] R. Berner, P. Lichtsteiner, and T. Delbruck, "Self-timed vertacolor dichromatic vision sensor for low power pattern detection," in *Circuits and Systems, 2008. IEEE International Symposium on*, 2008, pp. 1032 – 1035.

[11] T. Yoshikawa, Z. Tani, A. Aso, and H. Kawanabe, "Apparatus for sensing the wavelength and intensity of light," U.S. Patent 4 309 604, Jan. 1, 1982.

[12] R. F. Wolffenbuttel, "Color filters integrated with the detector in silicon," *IEEE Electron Device Letters*, vol. 8, pp. 13–15, 1987.

[13] C. Yuan, X. Zhihai, and F. Huajun, "A CMOS image sensor for monochromatic spectrum imaging," in *Imaging Systems and Techniques, 2009*, May 2009, pp. 6–10.

[14] J. Olsson and P. Hafliger, "Two color asynchronous event photo pixel," in *Circuits and Systems, 2008. IEEE International Symposium on*, May 2008, pp. 2146–2149.

[15] Z. Fu and A. H. Titus, "CMOS Neuromorphic Optical Sensor Chip With Color Change-Intensity Change Disambiguation," *IEEE Sensors Journal*, vol. 9, no. 6, pp. 689–696, 2009.

[16] G. Gilder, *The Silicon Eye: How a Silicon Valley Company Aims to Make All Current Computers, Cameras, and Cell Phones Obsolete*. W.W. Norton & Company, 2005.

[17] R. W. Rodieck, *The First Steps in Seeing*. Sinauer Associates, 1998.

[18] M. Sedjil, G. Lu, M. B. Chouikha, and A. Alexandre, "Modeling of BDJ and BTJ structures for color detection," *DTM99, SPIE*, vol. 3680, pp. 388–397, 1999.

[19] S. Liu, J. Kramer, G. Indiveri, T. Delbruck, and R. Douglas, *Analog VLSI: Circuits and Principles*. Cambridge, Massachusetts: The MIT Press, 2002.

[20] I. Brouk and Y. Nemirovsky, "Dimensional effects in CMOS photodiodes," *Solid-State Electronics*, vol. 46, no. 1, pp. 19 – 28, 2002.

[21] K. A. Boahen, "Point-to-point connectivity between neuromorphic chips using address events," *IEEE Trans. Circuits Syst. II, Analog Digit. Signal Process.*, vol. 47, no. 5, pp. 416–434, May 2000.